

HYP
2022
PRAGUE

14th International Conference on Hypernuclear and Strange Particle Physics
June 27 – July 1, 2022
Prague, Czech Republic

**Exploring the role of hyperons in high density matter
in the Quark-Meson-Coupling model**

J. R. Stone

Oxford/Tennessee



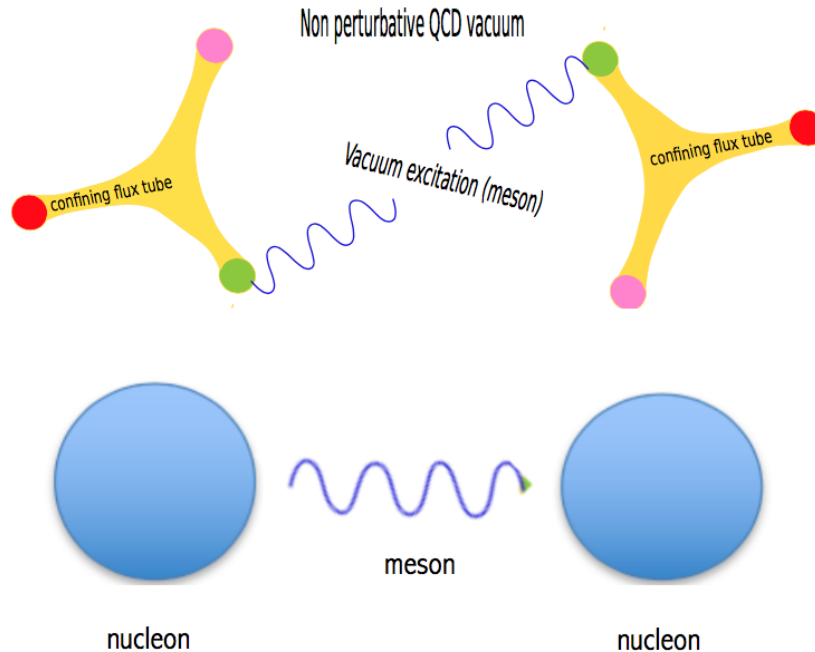
jirina.stone@physics.ox.ac.uk

Motivation:

**We do not know baryon-baryon interaction in medium
from first principles**

PS. We do not know it in free space either.....

A few remarks about the QMC model: Guichon1988, 1996,2004,Saito2007,Guichon2018



Baryon-baryon interaction takes place *self-consistently* between valence quarks, confined in overlapping baryons by exchange of virtual mesons.

The effect of dense medium surrounding the baryons, is modelled by dynamics of the quarks inside the individual particles.

Traditional models ignore internal structure of the nucleon and its dynamics

Construct a phenomenological relativistic mean field model for nuclear matter (and non-relativistic extension for finite nuclei)

Guichon, JRS, Thomas: Prog.Part.Nucl.Phys. 100,262(2018)

- Two pieces of physics:
- (i) MIT bag (confining potential)
 - (ii) meson fields: σ density dependent attractive
 ω and ρ repulsive

Total energy of a classical system of baryons at zero temperature, modeled as non-overlapping bags coupled to meson fields σ , ω and ρ is expressed as

$$E_{QMC} = \sum_{i=1, \dots} \sqrt{P_i^2 + M_i^2(\sigma(\vec{R}_i))} + g_\omega^i \omega(\vec{R}_i) + g_\rho \vec{I}_i \cdot \vec{B}(\vec{R}_i) + E_\sigma + E_{\omega, \rho},$$

$$M_i(\sigma) = M_i - w_{\sigma i} g_{\sigma N} \sigma + \frac{d}{2} \tilde{w}_{\sigma i} (g_{\sigma N} \sigma)^2,$$

Quantize and solved by traditional methods to calculate observables

Parameters (nuclear matter):

Data:

Nucleon–meson couplings in *free space*

$G_{\sigma N}$ $G_{\omega N}$ $G_{\rho N}$

ρ_0 E/A J

Mass of σ meson

700 MeV

Mass of ω and ρ

physical values

Bag radius

1 fm

Self energy of σ

0 MeV

$G_{\sigma N}$ $G_{\omega N}$ $G_{\rho N}$



are correlated

ρ_0 E/A J



$0.14 < \rho_0 < 0.17 \text{ fm}^{-3}$ (step 0.01)

$-15 < E/A < -17 \text{ MeV}$ (step 1)

$27 < J < 36 \text{ MeV}$ (step 1)

Observables used in the analysis:

Each observable is a function of three coordinates ρ_0 , E/A and J and cuts are made in the 3D space

- Slope of the symmetry energy L
- Volume incompressibility K
- Hyperon single particle potentials $U_\Lambda, U_\Sigma, U_\Xi$
- Cold EoS in the form E/A vs ρ
- Maximum gravitational mass and radius of cold NS
- Thresholds for appearance of hyperons (Λ must appear first)
- Direct URCA cooling mechanism (hyperons delay the cooling to higher densities)

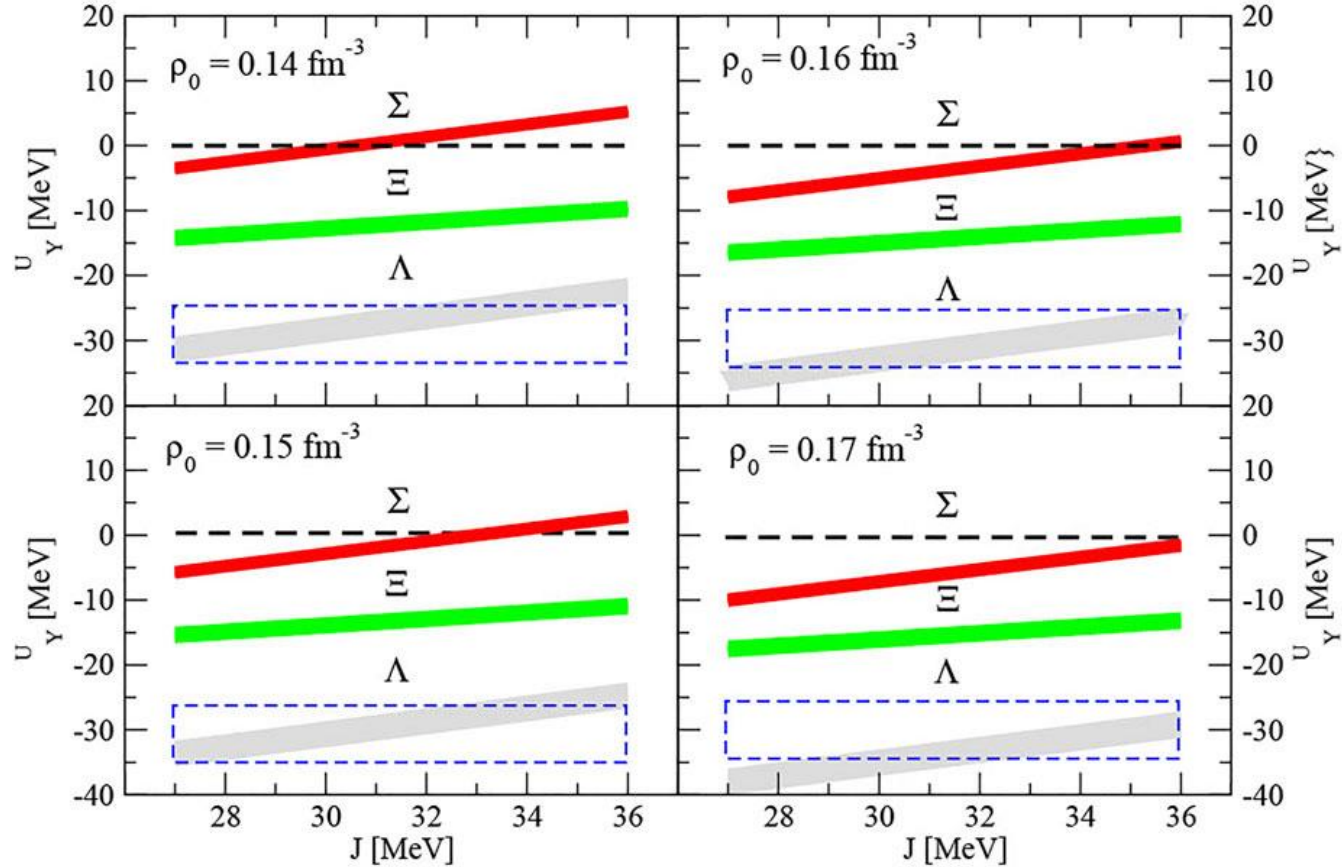
Results:

$$\rho_0 = 0.16 \text{ fm}^{-3}, E_0/A = -15 \text{ or } -16 \text{ MeV}, J = 31 \text{ MeV}$$

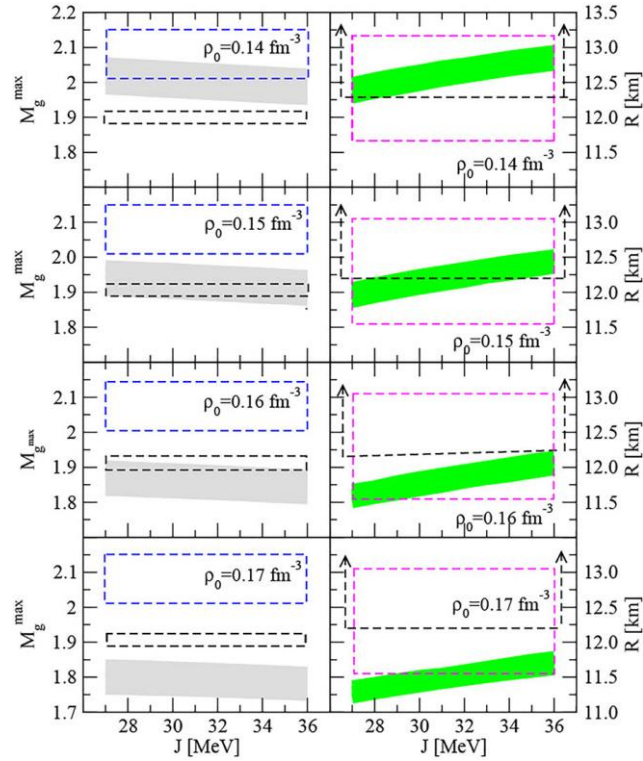
$$9.5 \leq G_\sigma \leq 10.0 \text{ fm}^2 \quad 5.8 \leq G_\omega \leq 6.1 \text{ fm}^2 \quad 3.35 \leq G_\rho \leq 3.45 \text{ fm}^2.$$

We find a weak dependence on J in most scenarios, in particular in NS.
The variation in E_0/A has less than 15% influence on most calculated quantities.

Single-particle potentials U_Λ (grey), U_Σ (red) and U_Ξ (green) as a function of J for $\rho_0 = 0.14, 0.15, 0.16$ and 0.17 fm^{-3} . The spread is due to uncertainty in E_0/A .



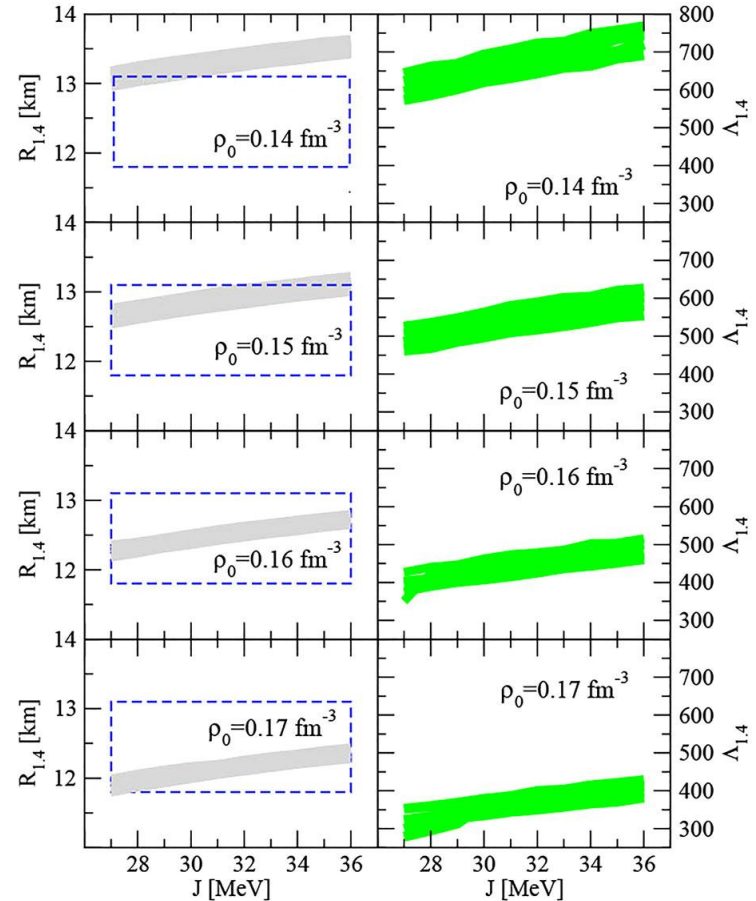
Maximum Gravitational mass and Radius



Left panel: The blue (black) dashed boxes PSR J0740 + 6620 (Fonseca et al., 2021) [PSR J1614-2230 (Arzoumanian et al., 2018)].

Right panel: The open black dashed boxes radius of the PSR J0740 + 6620 (Miller et al., 2021) reaching upper limit of 16.3 km. The magenta dashed box shows statistical analysis by (Miller et al., 2021).

Radius and tidal deformation of 1.4 M_{solar} NS

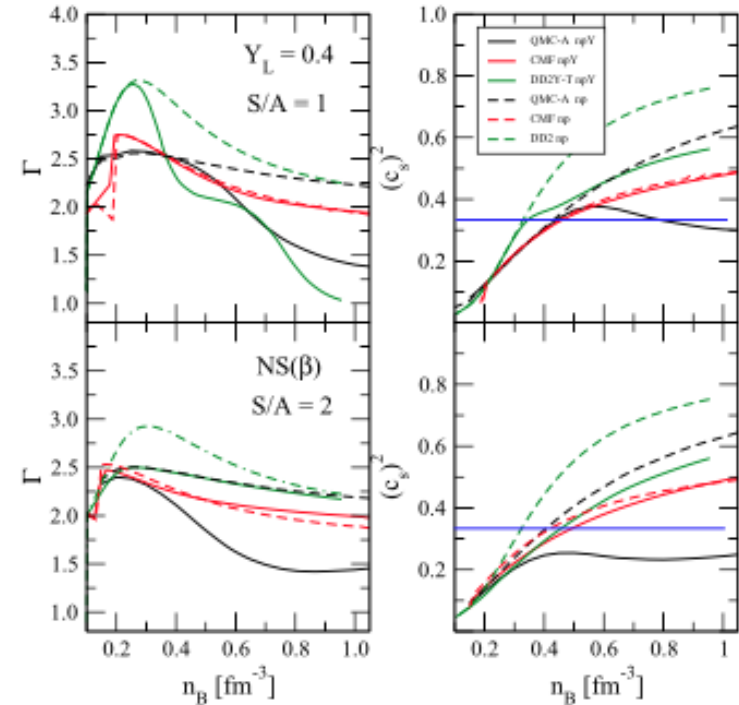
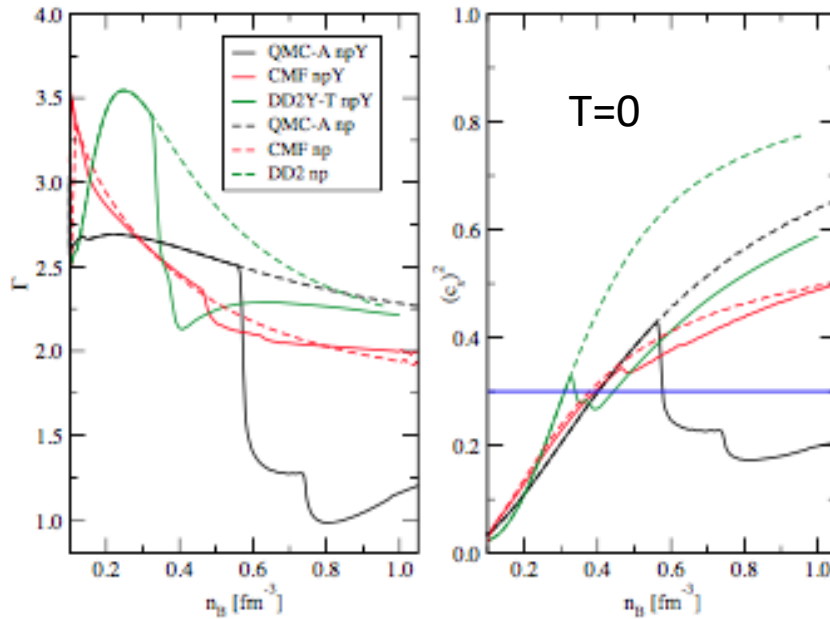


Left panel: Radii **Right panel:** tidal deformation

Adiabatic index and the speed of sound:

$$\Gamma = \frac{d \log P}{d \log n_B} = \frac{n_B}{P} \frac{dP}{dn_B}, \quad \text{Polytropic EoSs } \Gamma = 4/3 \text{ (5/3) for a relativistic (nonrel) free-Fermi gas.}$$

$$c_s^2 = \frac{dP}{d\epsilon}, \quad \text{Should be lower than the conformal limit } 1/3 \quad \text{Cherman, Cohen \& Nellore 2009}$$



Summary:

The concept of quark-meson coupling offers:

Fully relativistic mean field model of high density hyperonic matter
with a small number well constrained parameters forming a unique set (once determined)

Automatically includes many-body forces

Suitable for prediction of properties of neutron stars, supernovae and neutron star mergers
at zero and finite temperature

Treatment of finite nuclei (including superheavy) and hypernuclei with comparable success

No hyperon puzzle, the same parameters for nucleonic and hyperonic matter

Mechanism of saturation of nuclear forces

Calculation of hyperonic single particle potentials

Hartree-Fock method with full exchange (Fock) term included

But it is still a phenomenological model not solving the puzzle of baryon-baryon interaction either in free space or in medium.
We have to keep thinking.....

Binding of hypernuclei in the latest quark–meson-coupling model

Single-particle energies (in MeV) for ${}^{17}_Y\text{O}$, ${}^{41}_Y\text{Ca}$ and ${}^{49}_Y\text{Ca}$ hypernuclei. The experimental data are taken from Ref. [5, Table 11] for ${}^{16}_\Lambda\text{O}$ and from Ref. [33] for ${}^{40}_\Lambda\text{Ca}$.

	${}^{16}_\Lambda\text{O}$ (Expt.)	${}^{17}_\Lambda\text{O}$	${}^{17}_{\Sigma^0}\text{O}$	${}^{40}_\Lambda\text{Ca}$ (Expt.)	${}^{41}_\Lambda\text{Ca}$	${}^{41}_{\Sigma^0}\text{Ca}$	${}^{49}_\Lambda\text{Ca}$	${}^{49}_{\Sigma^0}\text{Ca}$
$1s_{1/2}$	$-12.42 \pm 0.05 \pm 0.36$	-16.2	-5.3	-18.7 ± 1.1	-20.6	-5.5	-21.9	-9.4
$1p_{3/2}$		-6.4	-		-13.9	-1.6	-15.4	-5.3
$1p_{1/2}$	$-1.85 \pm 0.06 \pm 0.36$	-6.4	-		-13.9	-1.9	-15.4	-5.6

The experimental data are taken from Ref. [5, Table 13].

	${}^{89}_\Lambda\text{Yb}$ (Expt.)	${}^{91}_\Lambda\text{Zr}$	${}^{91}_{\Sigma^0}\text{Zr}$	${}^{208}_\Lambda\text{Pb}$ (Expt.)	${}^{209}_\Lambda\text{Pb}$	${}^{209}_{\Sigma^0}\text{Pb}$
$1s_{1/2}$	-23.1 ± 0.5	-24.0	-9.9	-26.3 ± 0.8	-26.9	-15.0
$1p_{3/2}$		-19.4	-7.0		-24.0	-12.6
$1p_{1/2}$	-16.5 ± 4.1 (1p)	-19.4	-7.2	-21.9 ± 0.6 (1p)	-24.0	-12.7
$1d_{5/2}$		-13.4	-3.1	-	-20.1	-9.6
$2s_{1/2}$		-9.1	-	-	-17.1	-8.2
$1d_{3/2}$	-9.1 ± 1.3 (1d)	-13.4	-3.4	-16.8 ± 0.7 (1d)	-20.1	-9.8
$1f_{7/2}$		-6.5	-	-	-15.4	-6.2
$2p_{3/2}$		-1.7	-	-	-11.4	-4.2
$1f_{5/2}$	-2.3 ± 1.2 (1f)	-6.4	-	-11.7 ± 0.6 (1f)	-15.4	-6.5